Seismic low-frequency shadow detection based on the Levenberg-Marquardt reassignment operators using S-transforms

R. Anvarir[1, a,*], Adil Hussien Mohammed[2, b] and Shima Rashidi[3, c]

1 Faculty of Mining, Petroleum and Geophysics Engineering, Shahrood University of Technology, Shahrood, Iran.

2 Department of Communication and Computer Engineering, College of Engineering, Cihan University-Erbil, Iraq.

3 Department of Computer Science University of Human Development sulaymaniyah, Iraq.

E-mails: [a]rasoulanvarias93@email.com (Corresponding author) , [b]adil.mohammed@cihanuniversity.edu.iq , [c]shimarashidi6@gmail.com

ABSTRACT

Based on the phenomenon of low-frequency shadow beneath the oil and gas reservoirs, there is much theoretical research and practical production data. Therefore, accurate detection of the low-frequency shadow in order to predict reservoir. The high-precision detection time-frequency transform in this paper is achieved by adding Levenberg-Marquardt reassignment operators using S-transforms to adjust the window width adaptively according to the characteristics of different signal components. Finally, it optimizes the time-frequency distribution. Simulation results show that this method has a better time-frequency concentration than conventional methods. Finally, an application of this method in detecting low-frequency shadow verifies the effectiveness and feasibility, which provides a high-precision tool and means for reservoir prediction.

KEY WORDS: frequency resolution, detection, low-frequency shadow, shadow detection, upstream oil & gas, seismic low-frequency shadow detection,

1. INTRODUCTION

Hydrocarbon indicators widely have been studied by Seismic low-frequency shadows [1]. A low-frequency shadow (LFS) is a seismic reflection with a robust amplitude at low frequencies without delay beneath a hydrocarbon-bearing reservoir. Numerous LFSs examples of hydrocarbon indicators have been reported [2].

The seismic attenuation mechanism alone cannot be interpreted as a strong low-frequency amplitude anomaly zone near reservoirs [3], [11], [4]. Physical processes increased the strong amplitudes within the low-frequency anomalies. More than 10 causes that may lead to the generation of LFSs are listed by Ebrom (2004) [5], such as seismic data processing-related factors, attenuation and wave interferences. Quantifying the effects of seismic attenuation and stretching of normal moveout (NMO) on the generation of LFSs by numerical modelling of LFSs are used by Carcione et al. (2018) [6].

Time-frequency transforms have been widely used in seismic data processing and interpretations [7], [8]. The characteristics not effortlessly observed in the time representation or the frequency representation alone cannot be revealed by spectral decomposition. Because of the Heisenberg uncertainty principle and cross-terms, the conventional spectral decompositions such as short-time Fourier transform (STFT) and Wigner–Ville distribution (WVD) have some restrictions [2].

This paper used the Levenberg-Marquardt reassignment operators using S-transforms [12] spectrogram to overcome the mentioned restrictions. The resolution of a time-frequency representation using STFT is strongly dependent on the length of the window function. A short window length will result in a good time resolution, but a poor frequency resolution; a long window length will result in a poor time resolution but a good frequency resolution [9]. Therefore, a 2D deconvolution operator can be used to generate a high time-frequency representation of the signal with no cross-terms. The efficiency of this method is evaluated by applying it on both synthetic and real seismic data. The results of the synthetic example show that the Levenberg-Marquardt reassignment operators using S-transforms spectrogram has a fine resolution. Castagna et al. (2003) [10] used spectral decomposition to detect the low-frequency shadows associated with hydrocarbons. In fact, these shadows are often related to additional energy occurring at low frequencies rather than the preferential attenuation of higher frequencies. One possible explanation is that locally converted shear waves have travelled mostly as P-waves and thus arrive slightly after the true primary event. We used the Levenberg-Marquardt reassignment operators using S-transforms to illuminate the low-frequency shadow corresponding to a gas reservoir at one of the gas fields in the South West of Iran. The results of the real data example show that the proposed analysis has a much better resolution than the conventional spectral decomposition and can potentially be used to detect hydrocarbons from a gas reservoir directly using low-frequency shadows.

This study investigates the generation mechanism of the LFSs based on a field case in the Ordos Basin, which is situated in the Iran hydrocarbon fields. The paper is organized as follows. Section 2 describes **S- Transform**, **the Levenberg-Marquardt**

DOI: http://doi.org/10.24086/cocos2022/paper.632

reassignment operators using S-transforms. Some parts of the target horizon in the gas field show LFSs, but some parts do not have any LFSs. In section 3 we apply the proposed method on the synthetic model and real seismic LFSs of the study area on the frequency-dependent reflection coefficients related to the low-frequency shadows.

2. METHODOLOGY

2.1 S- Transform

Let define the S-transform as a particular case of the Short-Time Fourier Transform (STFT) using the window $g\left(t,\omega\right)=\frac{|\omega|}{\sqrt{2\pi}\omega_0 T}e^{-\frac{{\omega_0}^2 t^2}{2(\omega_0 T)^2}}$ [12]:

$$ST_x(t,\omega)\ =M_x(t,\omega)e^{j\Phi_x(t,\omega)}=\int x\left(\tau\right)g\left(t-\tau,\omega\right)e^{-j\omega\tau}d\tau$$

(1)

When we have:

$$\frac{\partial ST_x}{\partial\omega}\left(t,\omega\right)=\frac{\partial M_x}{\partial\omega}\left(t,\omega\right)e^{j\phi_x(t,\omega)}+j\frac{\partial\phi_x}{\partial\omega}\left(t,\omega\right)ST_x\left(t,\omega\right)$$

(2)

So finally we deduce

$$\frac{\partial\phi_x}{\partial\omega}\left(t,\omega\right)=\mathrm{Im}\left(\frac{\frac{\partial ST_x\left(t,\omega\right)}{\partial\omega}}{ST_x\left(t,\omega\right)}\right)=-t+\Re\mathrm{e}\left(\frac{ST_x^{\tau g}\left(t,\omega\right)}{ST_x\left(t,\omega\right)}\right)-\mathrm{Im}\left(\frac{\omega}{(\omega_0 T)^2}\frac{ST_x^{\tau^2 g}\left(t,\omega\right)}{ST_x\left(t,\omega\right)}\right)$$

(3)

We consider first the definition of the reassigned frequency coordinates and we compute **the reassignment operators using S-transforms as:**

$$\hat{t}\left(t,\omega\right)=t-\Re\mathrm{e}\left(\frac{ST_x^{\tau g}\left(t,\omega\right)}{ST_x\left(t,\omega\right)}\right) \quad (4)$$

And

$$\hat{\omega}\left(t,\omega\right)=\omega+\mathrm{Im}\left(\frac{ST_x^{Dg}\left(t,\omega\right)}{ST_x\left(t,\omega\right)}\right) \quad (5)$$

Where $Dg(t)\ =\frac{dg}{dt}\ (t)$ and the definition of the Levenberg-Marquardt reassignment operators

2.2 The Levenberg-Marquardt reassignment operators using S-transforms

Starting from the Stockwellogram classical reassignment operators, we have [12]:

$$\begin{pmatrix}\hat{t}\left(t,\omega\right)\\ \hat{\omega}\left(t,\omega\right)\end{pmatrix}=\begin{pmatrix}t\\ \omega\end{pmatrix}-\left(\nabla^t R_x\left(t,\omega\right)+\mu I_2\right)^{-1}R_x\left(t,\omega\right)$$

(6)

With

$$R_x\left(t,\omega\right)=\begin{pmatrix}t\\ \omega\end{pmatrix}-\begin{pmatrix}\hat{t}\left(t,\omega\right)\\ \hat{\omega}\left(t,\omega\right)\end{pmatrix} \quad)7($$

$$\nabla^t R_x\left(t,\omega\right)=\begin{pmatrix}\frac{\partial R_x}{\partial t}\left(t,\omega\right) & \frac{\partial R_x}{\partial\omega}\left(t,\omega\right)\end{pmatrix} \quad (8)$$

We directly obtain

$$R_x\left(t,\omega\right)=\begin{pmatrix}\Re\mathrm{e}\left(\frac{ST_x^{\tau g}\left(t,\omega\right)}{ST_x\left(t,\omega\right)}\right)\\ \mathrm{Im}\left(\frac{ST_x^{Dg}\left(t,\omega\right)}{ST_x\left(t,\omega\right)}\right)\end{pmatrix} \quad (9)$$

$$\nabla^t R_x\left(t,\omega\right)=\begin{pmatrix}\frac{\partial}{\partial t}\left[\Re\mathrm{e}\left(\frac{ST_x^{\tau g}\left(t,\omega\right)}{ST_x\left(t,\omega\right)}\right)\right] & \frac{\partial}{\partial\omega}\left[\Re\mathrm{e}\left(\frac{ST_x^{\tau g}}{ST_x}\right.\right.\\ -\frac{\partial}{\partial t}\left[\mathrm{Im}\left(\frac{ST_x^{Dg}\left(t,\omega\right)}{ST_x\left(t,\omega\right)}\right)\right] & -\frac{\partial}{\partial\omega}\left[\mathrm{Im}\left(\frac{ST_x^{Dg}}{ST_x}\right.\right.\end{pmatrix}$$

(10)

Therefore, the reassignment operator is an adaptive and invertible TFD that enhances the readability of the wavelet-based TF plane, utilizing frequency reassignment by shrinking the spectrum along the frequency axis. For nonlinear equations, Levenberg-Marquardt type algorithms were shown to have a quadratic rate of convergence if an appropriate error bound condition holds, see [14] **-**[17]**. So, The Levenberg-Marquardt algorithm is a classical method for solving nonlinear systems of equations that can come from various applications in engineering and economics.**

In the next section, we have first tested the performance of the Levenberg-Marquardt reassignment operators using S-transforms on synthetic signals contaminated by random noise. To investigate the generation mechanism of the LFSs based on a field case, we have applied the proposed method on it as trace by trace.

3. RESULTS

Here we consider a noisy synthetic signal that shows in fig 1a. For the evolution of the Levenberg-Marquardt reassignment operators using S-transforms, we have done a

DOI: http://doi.org/10.24086/cocos2022/paper.632

time-frequency map of it and the result has been compared with STFT (Figure 1b, 1c). As shown in figure 1, The Levenberg-Marquardt reassignment operators using S-transforms has a loser Reni factor than STFT and it demonstrates this transform has a good performance and is useful for non-linear and non-stationary signals. Renyi factor is another factor for more investigation of the proposed method. The **Renyi entropy of order** α **where** $\alpha \geq 0$ **and** $\alpha \neq 1$ **is defined as:**

$$H_{\alpha}(x) = \frac{1}{1-\alpha} \log\left(\sum_{i=1}^{n} p_i^{\alpha}\right) \tag{11}$$

Here, X **is a discrete random variable with possible outcomes in the set** $A = \{x_1, x_2, x_3, \ldots\ldots, x_n\}$ **and corresponding probabilities** $p_i \triangleq \Pr(X = x_i)$ **for** $i = 1,2,3,\ldots.n$. **The logarithm is conventionally taken to be base 2, especially in the context of information theory, where bits are used. If the probabilities are** $p_i = 1/n$ **then all the Renyi entropies of the distribution are equal to** $H_{\alpha}(x) = \log^{n}$. **In general, for all discrete random variables** X, $H_{\alpha}(x)$ **is a non-increasing function in** α. **The Renyi entropies for STFT and the proposed method are 8.9 and 6.16.**

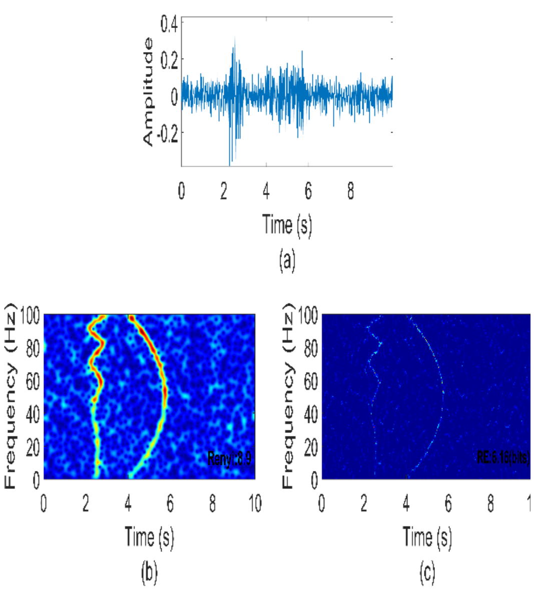

Figure 1. (a) Synthetic signal and (b), (c) time-frequency maps of the synthetic signal based on, STFT and proposed methods.

In addition to synthetic signals, the STFT and the Levenberg-Marquardt reassignment operators using S-transforms were all applied to real field data from one of the Iran hydrocarbon fields [see Figure 2].

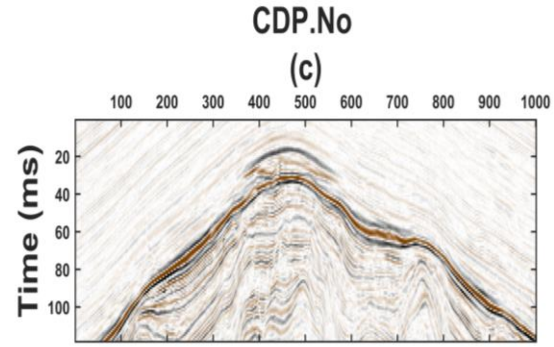

Figure 2. 2D real seismic data from an Iran hydrocarbon field.

The spectral decomposition method is a common time-frequency representation to find the low-frequency shadows associated with hydrocarbon. As it can be seen in Figure 3, the time-frequency map results of all two methods are shown in a position of the low-frequency shadow that the hydrocarbon is sited, then the frequency slices of 30 Hz and 60 Hz were detected. The window duration parameter for both methods is set to 0.001. Additionally, the Levenberg-Marquardt reassignment operators using S-transforms were able to depict the frequencies better with higher resolution. Thus, this method can be used to detect hydrocarbon using low-frequency shadows. Based on what is shown in Figure 3b, it was concluded that STFT does not have the potential capability of finding considerable frequency slices as the produced map is not clear and also has low resolution.

DOI: http://doi.org/10.24086/cocos2022/paper.632

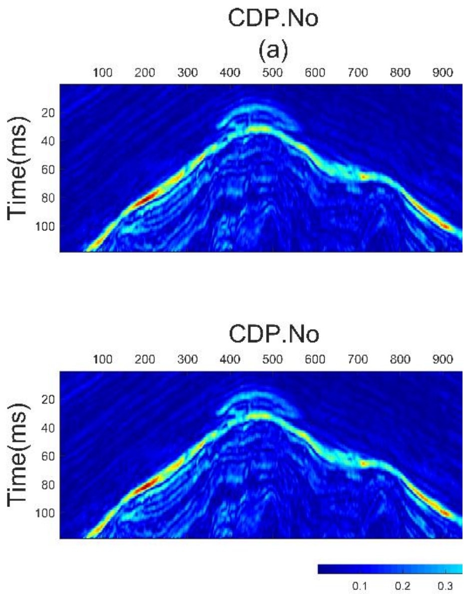

Figure 3. Time-frequency map of the field data based on, (a) STFT, (b) proposed methods,

4. CONCLUSIONS

We introduced a new higher resolution time-frequency transform called the Levenberg-Marquardt reassignment operators using S-transforms to detect low-frequency shadows associated with hydrocarbons, useful for non-linear and non-stationary signals. According to the consolidated mathematical background of this STFT transform and to illustrate its potential ability, we tested the proposed method with both synthetic and real field data and compared it with the STFT method. It was concluded that the Levenberg-Marquardt reassignment operators using S-transforms can detect the signals` components clearly and its noise background are commonly less than other STFT state-of-the-art method. The suggested method's application to both synthetic and seismic data show encouraging performance.

5. REFERENCES

I. References

[1] Goloshubin G., Van Shuyver C., Korneev V., Silin D., Vingalov V, "Reservoir imaging using low frequencies of seismic reflections," The Leading Edge, vol. 25, p. 527–531, 2006.

[2] Rasoul Anvari, Mohammad Amir Nazari Siahsar, Saman Gholtashi, Amin Roshandel Kahoo, Mokhtar Mohammadi, "Seismic random noise attenuation using synchrosqueezed wavelet transform and low-rank signal matrix approximation," EEE Transactions on Geoscience and Remote Sensing, vol. 55, no. 11, pp. 6574-6581, 2017.

[3] Taner, M. Turhan, Fulton Koehler, and R. E. Sheriff, "Complex seismic trace analysis," Geophysics, pp. 1041-1063., 1979.

[4] Y, Wang, "Frequencies of the Ricker wavelet, Geophysics," Geophysics, vol. 80, p. A31–A37, 2015.

[5] Ebrom D, "The low frequency gas shadow on seismic sections," The Leading Edge, vol. 23, p. 772. 2004.

[6] Carcione J. M., Qadrouh A., Perroud H., Gei D., Ba J., Picotti S, "Seismic attenuation, normal moveout stretch, and low-frequency shadows underlying bottom simulating reflector events," Geophysical Prospecting, vol. 66, p. 857–871, 2018.

[7] Rasoul Anvari, Amin Roshandel Kahoo, Mokhtar Mohammadi, Nabeel Ali Khan, Yangkang Chen, "Seismic random noise attenuation using sparse low-rank estimation of the signal in the time–frequency domain," IEEE Journal of Selected Topics in Applied Earth Observations and Remote Sensing, vol. 12, no. 5, pp. 1612-1618, 2019.

[8] M. M. A. R. K. N. A. K. A. I. A. Rasoul Anvari, "Random noise attenuation of 2D seismic data based on sparse low-rank estimation of the seismic signal," Computers & Geosciences, vol. 135, p. 104376, 2020.

[9] Boashash, B, "Time frequency signal: A comprehensive reference," Elsevier, 2003.

[10] F. F. P. G. P. L. O. Auger, "Time-frequency toolbox," CNRS, 1996.

[11] Castagna, J. P., Sun, S. and Siegfried, R. W, "Instantaneous spectral analysis: Detection of low-frequency shadows associated with hydrocarbons," The Leading, vol. 22, pp. 120-127, 2003.

[12] Yan Cao, Hayder A Dhahad, Hussein Togun, AS El-Shafay, Sagr Alamri, Ali A Rajhi, Ali E Anqi, Banar Fareed Ibrahim, "Development and transient performance analysis of a decentralized grid-connected smart energy system based on hybrid solar-geothermal resources; Techno-economic evaluation," Sustainable Cities and Society, vol. 76, p. 103425, 2022.

[13] Fourer, D., Auger, F., & Hu, J., "Reassigning and synchrosqueezing the Stockwell transform: Complementary proofs." 2015.

[14] J. Fan and Y. Yuan, "On the quadratic convergence of the LevenbergMarquardt method without nonsingularity assumption," Computing, vol. 74, no. 1, p. 23–39, 2005.

[15] A. Fischer, "Local behavior of an iterative framework for generalized equations," Mathematical Programming, vol. 94, no. 1, p. 91–124, 2002.

DOI: http://doi.org/10.24086/cocos2022/paper.632

[16] N. Yamashita and M. Fukushima, "On the rate of convergence of the Levenberg-Marquardt method. In Topics in numerical analysis," Springer, vol. 15, p. 239–249, 2001.

[17] J. Zhang, "On the convergence properties of the Levenberg-Marquardt method," Optimization, vol. 52, no. 6, and p:739–756, 2003.

DOI: http://doi.org/10.24086/cocos2022/paper.632